

## Effect of hafnium contaminant present in zirconium targets on sputter deposited ZrN thin films

D.A.R. Fernandez<sup>a,\*</sup>, B.S.S. Brito<sup>a</sup>, I.A.D. Santos<sup>a</sup>, V.F.D. Soares<sup>a</sup>, A.R. Terto<sup>a</sup>, G.B. de Oliveira<sup>a</sup>, R. Hubler<sup>b</sup>, W.W. Batista<sup>a</sup>, E.K. Tentardini<sup>a</sup>

<sup>a</sup> Universidade Federal de Sergipe, Av. Marechal Rondon, S/N, São Cristóvão, SE, Brazil

<sup>b</sup> Pontifícia Universidade Católica do Rio Grande do Sul – PUCRS, Av. Ipiranga, 6681 Porto Alegre, RS, Brazil

### ARTICLE INFO

#### Keywords:

ZrN  
Hafnium  
Inherent impurity  
Thin films

### ABSTRACT

Zirconium nitride thin films deposited by reactive magnetron sputtering recurrently present small amounts of hafnium (~1 at.%) in their composition derived from an inherent impurity existing in Zr targets. Hf presence in ZrN coatings is neglected by most of the researchers despite its known potential to modify properties of thin films. In this work, pure ZrN (0.9 at.% Hf contaminant) and ZrHfN thin films with intentional hafnium addition of 1.8, 3.7 and 5.5 at.% were deposited by reactive magnetron sputtering and characterized by RBS, GAXRD, SEM, nanohardness and high temperature oxidation tests. Based on the results, it is suggested that inherent hafnium presence in zirconium targets contributes for the good hardness values and oxidation resistance at 773 K registered for ZrN thin films.

### 1. Introduction

The unceasing technological development and the ever-increasing industrial demand subject materials to adverse service conditions. Thus, the necessity for new products and devices grow proportionally in several types of industries such as: electronic, optics, aeronautical, metallurgical, among others, justifying the need of continuous studies for development of new materials, as well as enhancement of existing materials.

During the last decades a great deal of advances has been made in the field of thin films, given their capacity to improve surface properties of components that present low lifespan or inferior performance when not coated [1–3]. In special, zirconium nitride (ZrN) thin films have attracted attention due to their high hardness and wear resistance [4,5], providing an increased performance to cutting tools and machining parts [6,7].

One of the main approaches to produce ZrN thin films is physical vapor deposition (PVD) method, in which reactive magnetron sputtering (RMS) plays a relevant role both academically and industrially [8]. However, it is known that targets used for this technique, in general, are not 100% pure, containing small amounts of impurities that commonly end up as a part of the chemical composition in many deposited coatings.

In this context, studies show a recurring content of hafnium in Zr and ZrN thin films deposited by RMS [9,10]. Due to the very low contamination (Hf < 1 at.%), detection of this chemical element is imperceptible by traditional characterization techniques, as EPMA [11] and EDS [12]. Even when Hf atoms are identified in ZrN matrix, their presence is still considered negligible [13,14].

Despite being registered that in small amounts chemical elements such as silicon and tantalum modify the microstructure and properties of ZrN coatings [15,16], the influence (positive or negative) of inherent Hf impurity on properties of ZrN thin films is scarce in literature.

The present work aims to evaluate the impact of inherent Hf presence in crystalline structure, hardness and oxidation resistance of ZrN thin films. By comparing usual ZrN thin films with a hypothetical Hf-free coating, researchers could infer whether inherent Hf impurity in ZrN harms the properties and, consequently, evaluate the need to produce more pure Zr targets.

Therefore, ZrN (0.9 at.% inherent Hf content) and ZrHfN thin films with intentional hafnium addition of 1.8, 3.7 and 5.5 at.% were deposited by reactive magnetron sputtering and had their properties compared. Coatings were characterized by Rutherford backscattering spectroscopy (RBS), glancing angle x-ray diffraction (GAXRD) before and after high temperature oxidation tests, nanohardness analyses and scanning electron microscopy (SEM).

\* Corresponding author at: Departamento de Ciência e Engenharia de Materiais, Universidade Federal de Sergipe, Av. Marechal Rondon, S/N, São Cristóvão, SE, Brazil.

E-mail address: [daniel.angel0275@gmail.com](mailto:daniel.angel0275@gmail.com) (D.A.R. Fernandez).

<https://doi.org/10.1016/j.nimb.2019.11.005>

Received 1 August 2019; Received in revised form 25 October 2019; Accepted 4 November 2019

Available online 14 November 2019

0168-583X/ © 2019 Elsevier B.V. All rights reserved.

## 2. Materials and methods

Thin films were deposited on polyethylene substrates for RBS analyses and on silicon substrates for GAXRD, SEM, nanohardness and oxidation tests. All substrates were cleaned by ultrasonic bath in distilled water and acetone for 20 min, being immediately dried and inserted in deposition chamber.

Magnetron sputtering deposition equipment AJA Orion 5-HV Sputtering Systems was used. For ZrN thin film a zirconium target was placed on a DC power supply while ZrHfN thin films were co-deposited adopting zirconium and hafnium targets connected to a DC and RF power supplies, respectively. Both targets have 50.8 mm diameter and 0.4 mm thickness.

All thin films were deposited using the same deposition parameters:  $1 \times 10^{-5}$  Pa base pressure,  $4 \times 10^{-1}$  Pa working pressure, Ar/N<sub>2</sub> gas flow of 19/2 sccm (with Ar and N<sub>2</sub> gases purity of 99.9999%). Zr target power was kept constant at 150 W, while Hf target was set at 150 W for pure HfN and 5, 25 and 35 W for ZrHfN coatings. Deposition time was set at 60 min for depositions on silicon substrates.

Thin films were characterized by RBS using alpha particles (He<sup>++</sup>) accelerated up to 1.8 MeV using 3 MV Tandetron equipment. For these analyses, depositions on polyethylene were carried out only for 6 min in order to achieve lower coating thicknesses (< 100 nm) aiming to avoid overlap of RBS peaks related to zirconium/hafnium and oxygen/nitrogen peaks.

Structural analyses and identification of present phases were investigated by GAXRD analyses. Shimadzu XRD 6000 equipment was used with incident angle of 1°, Cu-K $\alpha$  radiation ( $\lambda = 1.54 \text{ \AA}$ ), step of 0.02°, time per step of 0.006 s and  $2\theta$  from 20° to 80°. Nanohardness tests were executed with Fisherscope HV 100 nanoindenter, with Berkovich indenter and applied load of 5 mN.

Oxidation tests were performed in a muffle oven at 773 K and 873 K during 30 min with a heat rate of 10°/min. Afterwards samples were again analyzed by GAXRD with the same parameters mentioned previously. Morphology of the coatings after oxidation tests were accessed by SEM with a JEOL JCM 5700 microscope.

## 3. Results and discussion

### 3.1. RBS analyses

RBS analyses were performed in order to determine the content of N, Zr and Hf in the coatings. Polyethylene substrate was used aiming to favor the quantitative analysis of light elements such as nitrogen and oxygen. Fig. 1 shows RBS spectra obtained for pure ZrN (no intentional addition of hafnium) and the coating deposited with 35 W applied to Hf

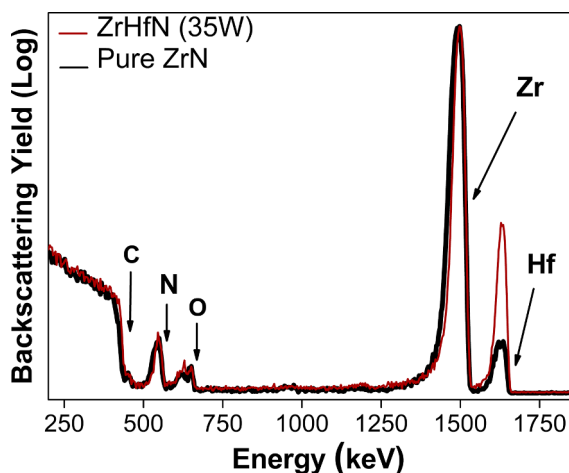


Fig. 1. RBS spectra for pure ZrN and ZrHfN with intentional Hf addition.

**Table 1**  
Chemical composition of ZrN and ZrHfN thin films.

Sample	Power in Hf target (W)	N (at.%)	Zr (at.%)	Hf (at.%)	(Hf/Zr + Hf)*100 (%)
ZrN	0	49.8	49.7	0.5	0.9
ZrHfN_1.8	5	55.6	43.6	0.8	1.8
ZrHfN_3.7	25	51.3	46.9	1.8	3.7
ZrHfN_5.5	35	51.4	45.9	2.7	5.5

target.

Peaks related to all chemical elements present in the films can be identified (zirconium, nitrogen and hafnium), as well as carbon from the polyethylene substrate. Despite rigorous cleaning procedures being employed, the high reactivity of O<sub>2</sub> and H<sub>2</sub>O molecules render inevitable residual oxygen presence as an impurity derived from chamber walls during deposition. The estimated oxygen concentration in the coatings, excluding the oxygen from the surface, was near to 8 at.% for all thin films, calculated by X-Rump software. Nevertheless, it is known that oxygen in low concentrations substitutes nitrogen in ZrN crystalline lattice, not altering its typical structure nor forming oxides [13,17].

Even with no intentional addition of hafnium, ZrN sample presents a peak related to this chemical element, ratifying its presence as an impurity derived from zirconium target. Table 1 shows the chemical composition of studied coatings disregarding oxygen presence and the adopted nomenclature based on Hf/(Zr + Hf) ratio.

### 3.2. GAXRD analyses

XRD patterns obtained for all samples are explicit in Fig. 2. Hafnium nitride (HfN) thin film has been analyzed in the present moment with comparative purposes only.

Through comparison with crystallographic data sheets ICDD PDF 35-0753 (ZrN) and ICDD PDF 65-0963 (HfN) it was verified that pure ZrN and HfN films presented a characteristic rock-salt nitride structure. Coincidentally, these two materials possess their planes growing at similar  $2\theta$  diffraction peaks. For ZrN, (1 1 1), (2 2 0) and (3 1 1) planes appear at 34°, 56.8° and 67.8°, respectively, whereas HfN shows a slight but noticeable difference mainly in (1 1 1) plane, which grows at 33.6°.

For ZrHfN thin films it can be observed that Hf addition resulted in the maintenance of ZrN matrix XRD patterns for all used hafnium contents, meaning the incorporation up to 5.5 at.% Hf probably did not promote the formation of new phases.

For all studied compositions, unaltered XRD patterns are observed due to similarities in lattice parameter of ZrN and HfN thin films and the low amount of Hf added. Given that fact, it can be suggested that HfN is completely dissolved in ZrN lattice and a solid solution was

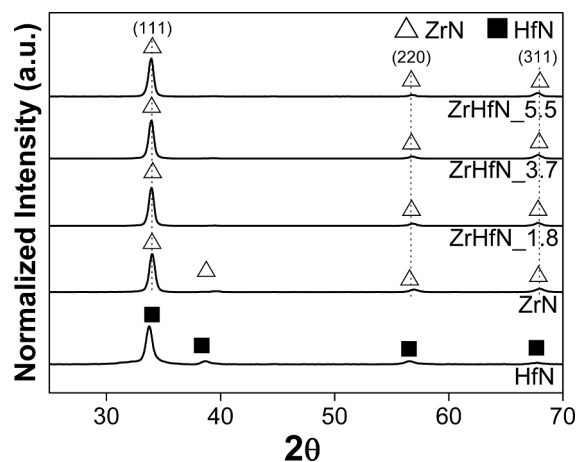


Fig. 2. XRD patterns of as deposited samples.

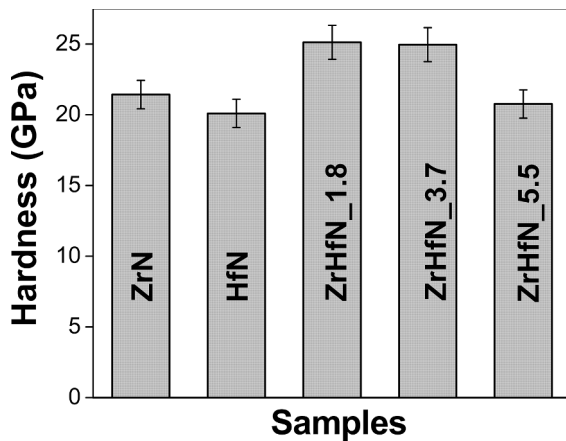


Fig. 3. Hardness values of all samples.

formed, which was observed earlier by other researchers [11,18,19].

The relative crystallite size for ZrN and ZrHfN samples was determined by Scherrer's equation using the FWHM value of (1 1 1) peaks. There was a gradual increase at the calculated grain sizes when Hf was added. While ZrN coating had an average crystallite size of 20.8 nm, both samples ZrHfN\_1.8 and ZrHfN\_3.7 had 24.5 nm and for ZrHfN\_5.5 coating the value increased to 27.8 nm.

Based on Fig. 2 results it is coherent to affirm that inherent hafnium presence in ZrN coatings deposited by magnetron sputtering does not modify significantly its crystalline structure, however, due to grain growth tendency some deviations on its microstructure are expected. Thus, hafnium impurity in the ZrN matrix may slightly influence some properties more sensitive to the presence of defects in a material, such as optical and electrical properties.

### 3.3. Nanohardness tests

Fig. 3 shows the hardness values obtained through nanohardness tests for all deposited samples. It can be observed that ZrN and HfN thin films presented hardness values of 21.4 and 20.1 GPa, respectively, coherent with values found in the literature [13,20].

Samples ZrHfN\_1.8 and ZrHfN\_3.7 showed similar hardness values of 25.1 and 24.9 GPa, respectively, corresponding to an increase of approximately 16% when compared to pure ZrN. On the other hand, when hafnium content was elevated to 5.5 at.% it was observed a decrease in hardness when compared to ZrHfN thin films with less Hf content, reaching an intermediate value of 20.7 GPa. Such value is an average to that obtained for ZrN and HfN, following the rules of mixtures.

Based on hardness results, it is suggested that in quantities inferior to 5.5 at.% solid solution hardening effect at ZrN matrix is predominant and promotes a considerable raise in hardness values. However, despite consisting of a solid solution as well, sample ZrHfN\_5.5 presented a grain growth superior to 14% in comparison to samples ZrHfN\_1.8 and ZrHfN\_3.7 grains. Such expressive raise in grain size is demonstrated to be a prevailing factor over solid solution effect, leading to the observed reduction in hardness values for sample with 5.5 at.% Hf.

It is therefore verified that hardness values of pure ZrN coatings are slightly improved by inherent presence of hafnium in Zr target, once small Hf contents (< 5.5 at.%) in ZrN matrix promote the solid solution strengthening when grain growth is not considerably expressive.

### 3.4. Oxidation tests

X-ray diffraction patterns obtained for all samples after exposure to 773 K are shown in Fig. 4. It is noted that ZrN thin film (0.9 at.% Hf contaminant) is majorly oxidized at 773 K, which is confirmed by the

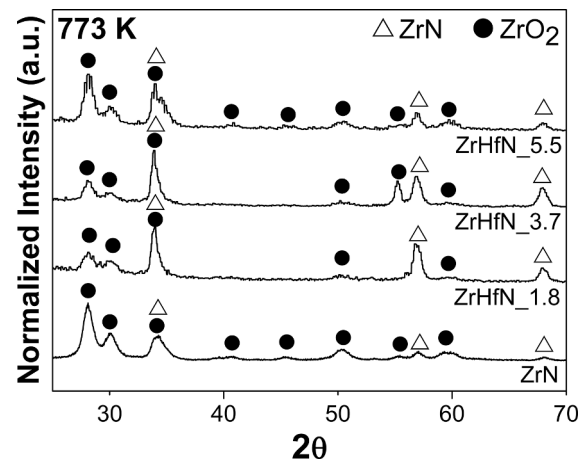


Fig. 4. GAXRD patterns for all samples after exposure to 773 K.

predominant presence of peaks related to its oxide ZrO<sub>2</sub>. Such behavior ratifies its low oxidation resistance in ~773 K, as previously discussed in literature [12].

For samples ZrHfN\_1.8 and ZrHfN\_3.7, it is observed that peaks related to ZrN have their intensity maintained after exposure to 773 K when compared to pure ZrN pattern, showing less peaks related to zirconium oxides as well. On the other hand, sample with 5.5 at.% Hf presented a reduction of intensity in ZrN peaks while ZrO<sub>2</sub> peaks are more pronounced.

These results follow the same behavior observed for nanohardness analyses: samples ZrHfN\_1.8 and ZrHfN\_3.7 presented an improved performance when compared to pure ZrN while decay can be observed for sample ZrHfN\_5.5. Thus, in a first moment the hafnium atoms present in solid solution ZrN structure reinforce it and improve its resistance to high temperatures. Nevertheless, in ZrHfN\_5.5 sample there is a visible grain growth, responsible to eliminate the improvement obtained by the solid solution effect and reaching results equivalent to those registered for pure ZrN.

Thus, it can be inferred that small hafnium content present in Zr targets positively contributes to oxidation resistance at 773 K for sputtered ZrN thin films. Aiming to further investigate the permanence of ZrN peaks in high temperatures, a second oxidation test was carried out at 873 K. Fig. 5 shows x-ray diffraction patterns for all oxidized samples.

Only peaks related to zirconium oxide can be identified in all patterns, indicating the complete oxidation of coatings at such temperature. Given that ZrN thin film at 773 K was oxidized, the same behavior was expected to be repeated also at 873 K, fact that occurred despite the

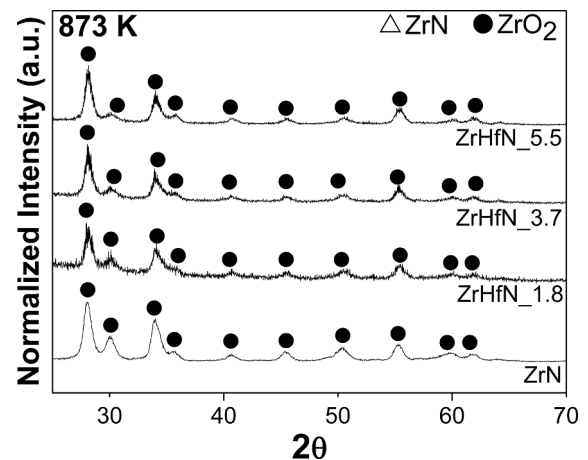


Fig. 5. GAXRD patterns for all samples after exposure to 873 K.

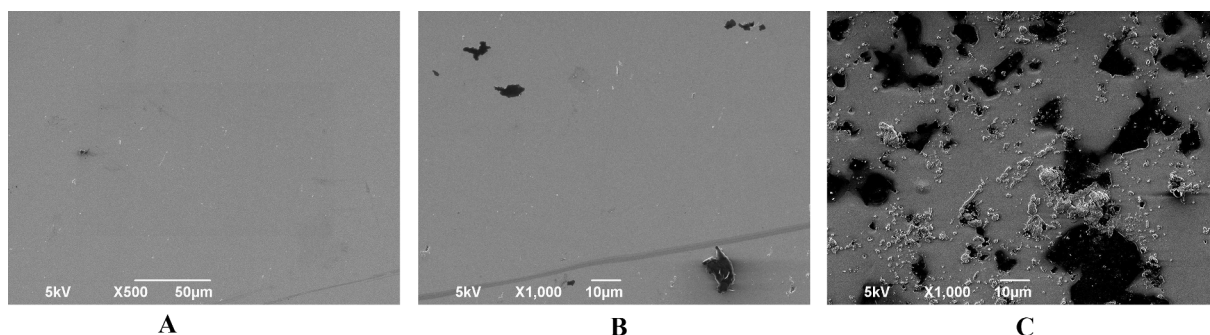


Fig. 6. SEM images obtained for sample ZrHfN\_1.8 (a) as deposited, (b) after oxidation test at 773 K and (c) after oxidation test at 873 K.

addition of Hf up to 5.5 at.%. It is verified therefore that Hf inherent impurity does not alter oxidation resistance of ZrN thin films at 873 K and above.

### 3.5. SEM analyses

SEM images of all samples were registered before and after oxidation tests in order to better analyze the behavior discussed in GAXRD patterns. All samples presented images with similar aspects, thus only images related to one sample is showed as a reference. Fig. 6a presents the micrograph obtained by SEM for as deposited ZrHfN\_1.8 sample. It is possible to observe that this sample is characterized with a homogeneous and defects-free surface. Similar surfaces were observed for all as deposited samples. Those features are a consequence of substrate cleaning procedures performed before depositions and magnetron sputtering technique itself. It was not possible to determine the grain size of samples by SEM analyses.

Fig. 6b reveals a homogeneous surface, though with the presence of some bubbles in samples ZrHfN\_1.8. It evidences that despite the presence of ZrN phase previously seen by GAXRD for this sample, the formation of ZrO<sub>2</sub> probably released nitrogen from original matrix. When exposed to high temperatures, zirconium nitride is dissociated, resulting in free Zr and N atoms. Zirconium reacts with oxygen, originating ZrO<sub>2</sub> seen by GAXRD and N atoms form N<sub>2</sub> gaseous molecules, which are expelled to the atmosphere and cause the formation of bubbles.

This process is intensified with the raise in temperature, as seen in Fig. 6c. Complete oxidation identified for these samples by GAXRD reflect a morphology with high levels of degradation due to intense and harsh nitrogen gas release.

## 4. Conclusions

The influence of hafnium concentration in ZrN and ZrHfN thin films was investigated in this work. Modification of crystalline structure cannot be observed by GAXRD due to formation of a solid solution, nonetheless, hafnium addition promotes a ZrN grain growth even in small quantities, calculated by Scherer's formula.

ZrHfN\_1.8 and ZrHfN\_3.7 thin films presented the highest hardness values in this study, however, for sample ZrHfN\_5.5 the values returned to those of pure ZrN. Initially, Hf in solid solution was responsible for the increment in hardness, but with 5.5 at.% Hf grain growth phenomenon determined the decrease in hardness, even with Hf remaining in solid solution. A better behavior for samples up to 3.7 at.% Hf was also identified for oxidation tests at 773 K, but at 873 K all samples were completely oxidized, registering increase in size and quantity of bubbles when temperature was elevated from 773 K to 873 K.

Based on the presented results it is assumed that inherent hafnium atoms presence in pure ZrN thin films (0.9 at.% Hf) seem to influence grain size, hardness and oxidation resistance of ZrN coatings. For metal mechanical applications, this small hafnium content can act positively.

However, other chemical and physical properties as optical and electrical variables must be studied to observe the positive/negative influence of this contamination in ZrN coatings in other to ascertain the necessity of producing zirconium targets with higher degree of purity for PVD deposition processes.

### Declaration of Competing Interest

The authors declare that they have no known competing financial interests or personal relationships that could have appeared to influence the work reported in this paper.

### Acknowledgments

The authors would like to thank the UFRGS Ionic Implantation Laboratory for RBS analyses and CNPQ, CAPES and FAPITEC/SE for financial support.

### References

- [1] K. Benouareth, P. Tristant, C. Jaoul, C.L. Niniven, C. Nouveau, C.D. Tixier, A. Bouabellou, Study of the interaction between a zirconium thin film and an EN C100 steel substrate: temperature effect, *Vacuum* 125 (2016), <https://doi.org/10.1016/j.vacuum.2015.11.002>.
- [2] K. Seshan, *Handbook of thin film deposition processes and techniques*, Andrew Publishing (2002).
- [3] K. Wasa, M. Kitabatake, H. Adachi, *Thin films materials technology: Sputtering of compound materials*, Springer, 2004.
- [4] B. Abdallah, M. Naddaf, M. A-Kharroub, Structural, mechanical, electrical and wetting properties of ZrNx films deposited by Ar/N<sub>2</sub> vacuum arc discharge: effect of nitrogen partial pressure, *Nucl. Instrum. Methods Phys. Res., Sect. B* 298 (2013), <https://doi.org/10.1016/j.nimb.2013.01.003>.
- [5] K. Mahmood, S. Bashir, M. Faizan-ul-Haq, A. Akram, M.S. Hayat, A. Mahmood Rafique, Surface, structural, electrical and mechanical modifications of pulsed laser deposited ZrN thin films by implantation of MeV carbon ions, *Nucl. Instrum. Methods Phys. Res., Sect. B* 448 (2019), <https://doi.org/10.1016/j.nimb.2019.04.013>.
- [6] K. Han, G. Lin, C. Dong, K. Tai, X. Jiang, Experimental study on atomic-scale strengthening mechanism of the IVB transition-metal nitrides, *J. Alloy. Compd.* 696 (2017), <https://doi.org/10.1016/j.jallcom.2016.11.329>.
- [7] B. Wang, V. Tomar, A. Haque, In-situ TEM mechanical testing of nanocrystalline zirconium thin films, *Mater. Lett.* 152 (2015), <https://doi.org/10.1016/j.matlet.2015.03.105>.
- [8] R.P. Howson, Synthesis of sputtered thin films in low energy ion beams, *Nucl. Instrum. Methods Phys. Res., Sect. B* 121 (1997), [https://doi.org/10.1016/s0168-583x\(96\)00370-9](https://doi.org/10.1016/s0168-583x(96)00370-9).
- [9] F.G.R. Freitas, R. Hübler, G. Soares, A.G.S. Conceição, E.R. Vitória, R.G. Carvalho, E.K. Tentardini, Structural and mechanical properties of Zr-Si-N thin films prepared by reactive magnetron sputtering, *Mater. Res.* 18 (2015), <https://doi.org/10.1590/1516-1439.336214>.
- [10] E.G. Njoroge, C.C. Theron, J.B. Malherbe, O.M. Ndwandwe, Kinetics of solid-state reactions between zirconium thin film and silicon carbide at elevated temperatures, *Nuclear Instruments and Methods in Physics Research B* 332 (2014), <https://doi.org/10.1016/j.nimb.2014.02.047>.
- [11] Z.T. Wu, Z.B. Qi, D.F. Zhang, Z.C. Wang, Microstructure, mechanical properties and oxidation resistance of (Zr, Hf)N<sub>x</sub> coatings by magnetron co-sputtering, *Surf. Coat. Technol.* 276 (2015), <https://doi.org/10.1016/j.surfcoat.2015.06.071>.
- [12] W.Z. Li, H.W. Liu, M. Evaristo, T. Polcar, A. Cavaleiro, Influence of Al content on the mechanical properties and thermal stability in protective and oxidation atmospheres of Zr–Cr–Al–N coatings, *Surf. Coat. Technol.* 236 (2013), <https://doi.org/10.1016/j.surfcoat.2013.09.052>.

- [13] P.C. Silva Neto, F.G.R. Freitas, D.A.R. Fernandez, R.G. Carvalho, L.C. Felix, A.R. Terto, R. Hubler, F.M.T. Mendes, A.H. Silva Junior, E.K. Tentardini, Investigation of microstructure and properties of magnetron sputtered Zr-Si-N thin films with different Si content, *Surf. Coat. Technol.* 353 (2018), <https://doi.org/10.1016/j.surfcoat.2018.07.106>.
- [14] V.F.D. Soares, D.A.R. Fernandez, A.S. Fontes Junior, R.G. Carvalho, R. Machado, F.M.T. Mendes, E.K. Tentardini, Structure and high temperature oxidation of  $Zr_{(1-x)}Mo_xN$  thin films deposited by reactive magnetron sputtering, *Appl. Surf. Sci.* 285 (2019), <https://doi.org/10.1016/j.apsusc.2019.04.238>.
- [15] T. Mae, M. Nose, M. Zhou, T. Nagae, K. Shimamura, The effects of Si addition on the structure and mechanical properties of ZrN thin films deposited by and r.f. reactive sputtering method, *Surf. Coat. Technol.* 142 (2001), [https://doi.org/10.1016/S0257-8972\(01\)01187-2](https://doi.org/10.1016/S0257-8972(01)01187-2).
- [16] J.L. Ruan, J.L. Huang, H.H. Lu, J.S. Chen, D.F. Lii, Effects of the Ta content on the microstructure and electrical property of reactively sputtered  $Ta_xZr_{1-x}N$  thin films, *Thin Solid Films* 519 (2011), <https://doi.org/10.1016/j.tsf.2011.01.066>.
- [17] M.A. Signore, A. Rizzo, L. Mirengi, M.A. Tagliente, A. Cappello, Characterization of zirconium oxynitride films obtained by radio frequency magnetron reactive sputtering, *Thin Solid Films* 515 (2007), <https://doi.org/10.1016/j.tsf.2007.02.033>.
- [18] E. Atar, C. Sarioglu, H. Cimenoglu, E.S.Kayali, Residual stresses in (Zr,Hf)N films (up to 11.9 at.% Hf) measured by X-ray diffraction using experimentally calculated XECs. *Surface Coatings Technol.* v191, 2005. <https://doi.org/10.1016/j.surfcoat.2004.02.024>.
- [19] E. Atar, E. Kayali, H. Cimenoglu, Reciprocating wear behaviour of (Zr, Hf)N coatings, *Wear* 257 (2004), <https://doi.org/10.1016/j.wear.2004.03.005>.
- [20] W. Tillmann, N.F.L. Dias, D. Stangier, M. Tolan, M. Paulus, Structure and mechanical properties of hafnium nitride films deposited by direct current, mid-frequency, and high-power impulse magnetron sputtering, *Thin Solid Films* 669 (2019), <https://doi.org/10.1016/j.tsf.2018.10.035>.